Korea-Australia Rheology Journal
Vol. 14, No. 2, June 2002 pp. 63-70

Effects of chemical reaction on the polishing rate and surface planarity in the copper CMP

Sun Hyuk Bae, Seung-Man Yang and Do Hyun Kim*
Center for Ultramicrochemical Process Systems, Department of Chemical and Biomolecular Engineering
Korea Advanced Institute of Science and Technology, Daejeon 305-701, Korea
(Received, May 1, 2002)

Abstract

Chemical mechanical planarization (CMP) is the polishing process enabled by both chemical and mechanical actions. CMP is used in the fabrication process of the integrated circuits to achieve adequate planarity necessary for stringent photolithography depth of focus requirements. And recently copper is preferred in the metallization process because of its low resistivity. We have studied the effects of chemical reaction on the polishing rate and surface planarity in copper CMP by means of numerical simulation solving Navier-Stokes equation and copper diffusion equation. We have performed pore-scale simulation and integrated the results over all the pores underneath the wafer surface to calculate the macroscopic material removal rate. The mechanical abrasion effect was not included in our study and we concentrated our focus on the transport phenomena occurring in a single pore. We have observed the effects of several parameters such as concentration of chemical additives, relative velocity of the wafer, slurry film thickness or aspect ratio of the pore on the copper removal rate and the surface planarity. We observed that when the chemical reaction was rate-limiting step, the results of simulation matched well with the experimental data.

1. Introduction

Chemical mechanical planarization (CMP) is a polishing process performed by the chemical and mechanical actions. CMP is currently being used in the fabrication of integrated circuits and has been identified as an enabling technology for establishing reliable multilevel interconnects.

In a typical CMP machine, a wafer is mounted on a wafer carrier and is rubbed against a polishing pad under a load with a rotary motion in the presence of slurry. Wafer carrier and pad are rotated with same angular velocity for the uniform distribution of relative velocity on the wafer surface. The slurry which contains a colloidal suspension of abrasive particles such as alumina or silica and specific chemical additives is distributed throughout the pad and enhances the chemical and mechanical action between the wafer and the pad. Polishing pad made of polymeric material (e.g. polyurethane) has porous surface where chemical reaction between the slurry and the wafer occurs.

Most current IC metallization schemes utilize aluminum alloys as the interconnect metal. But lower resistivity material has been investigated to reduce the interconnection time delay because it increases steeply as feature size decreases. While aluminum is considered good conductor with a resistivity of 2.66 μΩ-cm, copper possesses even lower resistivity which is 1.67 μΩ-cm. Therefore copper has been selected as a new material for metallization and it leads to the adoption of copper CMP in semiconductor fabrication processes (Steigerwald *et al.*, 1997).

The basic model of polishing was investigated by Preston (1927). He proposed the polishing rate of material to be proportional to a load and relative velocity. Cook (1990) reviewed the modeling of glass polishing and provided the mechanism by which the material is removed. Cook suggests that polishing occurs due to the softening of glass surface by the chemicals and subsequent mechanical abrasion of this softened layer by abrasive particles.

The first work dealing with the fundamental aspect of CMP was performed by Runnels *et al.* (Runnels, 1994; Runnels; 1996; Runnels and Eyman, 1994). They constructed the fluid mechanical model for the flow of slurry between the pad and the wafer. They proposed several models accounting for the stress in the polishing pad and the fluid flow as well as the removal of material by erosion. They solved the steady Navier-Stokes equation for the slurry flow with no-slip boundary condition on the surfaces of pad and wafer. The main results from this model were the slurry film thickness and shear stress on the wafer sur-

*Corresponding author: dokim@kaist.ac.kr

face. They used additional empirical model to relate the polishing rate to the shear stress on the wafer surface, so that the polishing rate of material is proportional to the shear stress. As a result of surface removal, time-dependent evolution of surface shape was predicted, while film thickness was in the range of 10 to 50 μm.

Many experiments were performed to investigate the thickness of slurry film. Levert *et al.* (1998) suggested the slurry film thickness comparable to the diameter of particles caught between pad and wafer. This result is consistent with that of Bhushan *et al.* (1995) who performed oxide CMP. In his experiment, the polishing rate was nearly zero when the gap between the wafer and the pad was fixed and much larger than the average particle diameter. But when the gap distance was reduced to be equal or smaller than particle diameter, the wafer started to be polished and the polishing rate was varied by the process parameters such as a load or relative velocity. In our study we used the concept of Levert *et al.* and Bhushan *et al.* for the film thickness.

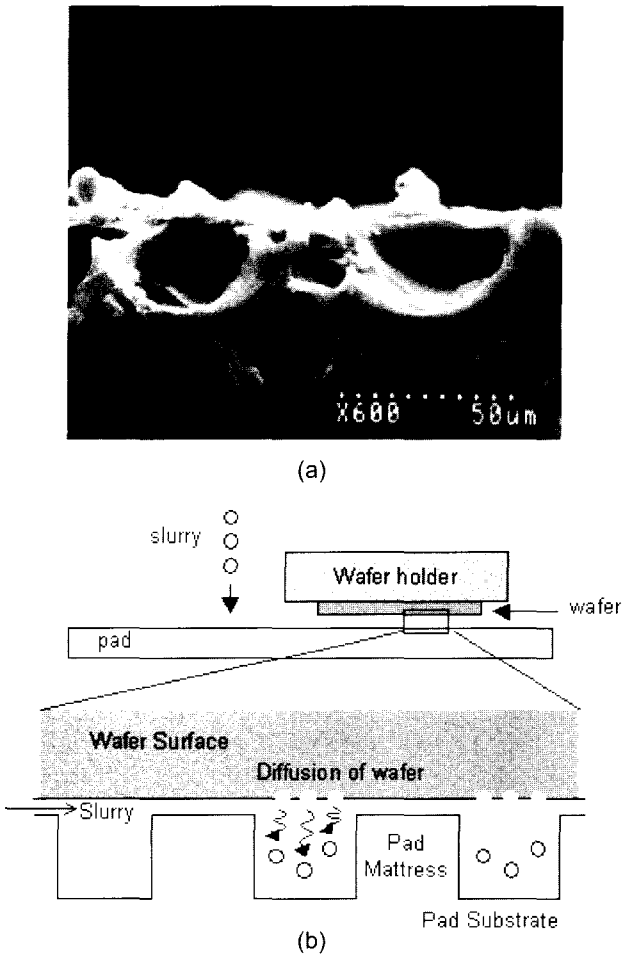

Fig. 1. (a) Cross-sectional SEM image of IC1000. (b) Schematic of the repeating cell model of the pad in a magnified view of a small region between the wafer and the pad.

2. Physical description of the model

In a typical CMP process, IC 1000 of Rodel, Inc. is usually used as a polishing pad. Fig. 1(a) shows the cross-sectional SEM image of IC 1000. According to Subramanian *et al.* (1999), the size and shape of pores can be assumed to be regular, which is useful in the fundamental step of CMP modeling.

Mechanical abrasion between the particles and the wafer occurs in the upper pad areas where the particles are in contact with wafer. In this study we did not include the mechanical abrasion effect and concentrated our focus to the chemical action of polishing. The polishing pad is assumed to be composed of many repeated unit cells as shown in Fig. 1(b). By analyzing the transport of material in a unit cell, macroscopic prediction of material removal rate can be made by integrating over the cells underneath the wafer. This concept is shown in Fig. 2 which is a plane view of a wafer with a unit cell in a pad. When we set the coordinate system on the wafer, the cell would traverse under the wafer along a strip with a width of dz. The chemical additives in the slurry in the unit cell will react with the wafer surface while the cell travels to the end of the strap. Therefore the removal rate along the strap due to the chemical reaction could be predicted by integrating the removal rate in a single unit cell over the exposure time. Also we can predict the removal rate in the whole wafer surface by integrating that in the straps along z-direction. Before the cell enters under the wafer, the cell is assumed to have no dissolved copper materials in the slurry. And the dissolved copper material diffuses from the wafer surface into the slurry by means of the concentration gradient and the slurry flow. This process is not steady because the concentration distribution of the dissolved copper changes depending on the position of unit cell along a strap. In other words, it depends on the exposure time. This concentration fields could be modeled using an unsteady conservation equation of dissolved copper, along with suitable boundary conditions. Before analyzing mass transfer, it is

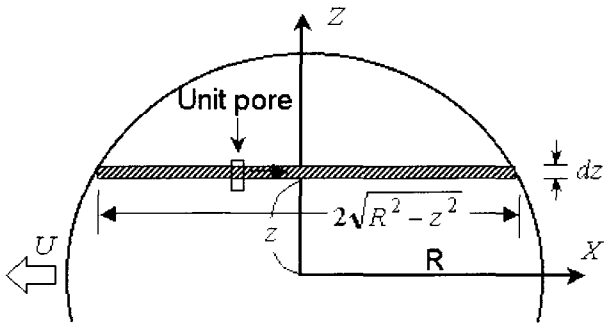

Fig. 2. Schematic of a wafer with a unit cell in a pad. Wafer moves with the velocity V and the unit cell is exposed to neighboring wafer surface.

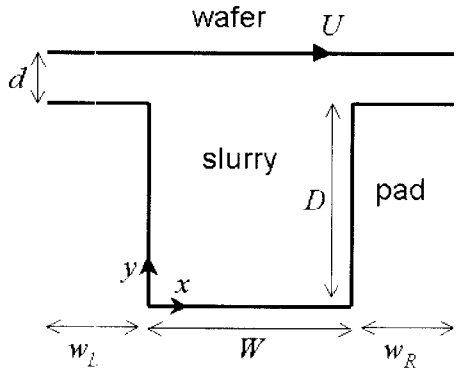

Fig. 3. Schematic of a numerical domain representing a pore in a pad.

necessary to have a detailed knowledge of the velocity field within the unit cell. The velocity field under the wafer also varies with exposure time but we found that the velocity field reaches steady-state just within very short time. Therefore, we assumed that the velocity field is constant throughout the total exposure time.

3. Theoretical development and numerical method

The model is two-dimensional and the pore is modeled as a rectangular shape with equal depth D and width W of 30 μm as shown in Fig. 3. We assume no variation in the z-direction normal to the plane of the paper. The thickness of slurry film is same to the size of particle diameter which is order of 0.3 μm or less, even though the agglomerated particles exist. Therefore the thickness of slurry film d is assumed as 300 nm in our study. The length of slits, w_L and w_R are half the width of the cavity, which is based on the TEM image of IC 1000 shown in Fig. 1(a). The origin of coordinates is chosen at the left bottom corner of the cavity. The liquid is assumed to be an incompressible Newtonian fluid and the physical properties are assumed to be constant in the pore.

The velocity field in a unit pore can be obtained by solving the following dimensionless continuity and Navier-Stokes equations:

$$\frac{\partial u}{\partial x}+\frac{\partial v}{\partial y}=0 \tag{1}$$

$$Re\left(u\frac{\partial u}{\partial x}+v\frac{\partial u}{\partial y}\right)=-\frac{\partial P}{\partial x}+\frac{\partial^2 u}{\partial x^2}+\frac{\partial^2 u}{\partial y^2} \tag{2}$$

$$Re\left(u\frac{\partial v}{\partial x}+v\frac{\partial v}{\partial y}\right)=-\frac{\partial P}{\partial y}+\frac{\partial^2 v}{\partial x^2}+\frac{\partial^2 v}{\partial y^2} \tag{3}$$

where $x=\tilde{x}/W$, $y=\tilde{y}/W$, $u=\tilde{u}/V$, $v=\tilde{v}/V$ and $P=\tilde{P}/P_c$. The relative velocity of wafer, V, varies from 0.1 to 1.0 m/s in a typical CMP process and the characteristic pressure P_c is $\mu V/W$. The Reynolds number is defined as

Table 1. Material properties and process parameters

	Parameters	Values
ρ	Density of slurry	1.05 g/cm^3
ρ_{cu}	Density of copper	8.99 g/cm^3
μ	Viscosity of slurry	2.14 cP
D_{cu}	Diffusivity of copper	1.81×10^{-9} m^2/sec
MW_{cu}	Molecular weight of copper	63.55 g/mol
V	Velocity of wafer	0.1~1.3 m/s
D	Depth of pore	30 μm
W	Width of pore	30 μm
d	Slurry film thickness	300 nm
K_{eq}	Equilibrium constant of reaction	4.23×10^{-5} /mol
C_N	Concentration of ammonia	1~3 vol.%
C_F	Concentration of Ferricyanide	1~5 wt.%

$$Re=\frac{\rho VW}{\mu} \tag{4}$$

Material properties and process parameters are listed in the Table 1. We applied no-slip condition on the wafer and pad surface and the x direction velocity on the wafer surface is V. At both inlet and outlet boundary, $\partial u/\partial x=0$ and $v=0$.

The chemical reaction between the wafer material and the chemical additives in slurry occurs on the wafer surface. This reaction is suggested by Sainio *et al.* (1996) where copper in ammonia-based slurries dissolves to form a cuprous diamine complex $Cu(NH_3)_2^+$. The dissolution reaction of copper by the slurry is

$$Cu+Fe(CN)_6^{3-}+2NH_3 \overset{K_{eq}}{\longleftrightarrow} Cu(NH_3)_2^{+}+Fe(CN)_6^{4-} \tag{5}$$

where K_{eq} is the equilibrium constant for the reaction with a value of 4.225×10^{-5} /mol (Sainio *et al.*, 1996; Sundararajan *et al.*, 1999). It is assumed that reaction (5) is fast and attains quickly to equilibrium at the wafer surface. Then, the equilibrium concentration of the dissolved copper species, $Cu(NH_3)_2^+$, at the wafer surface, C_s, is given by

$$C_s=\sqrt{K_{eq}}\sqrt{C_F C_N} \tag{6}$$

where C_F is the concentration of potassium ferricyanide and C_N is the concentration of ammonium hydroxide in the slurry. Both, C_F and C_N are assumed to be uniform in the slurry. The dissolved copper species diffuses from the wafer surface and is carried away by convective motion of slurry. The transport equation can be written for the copper concentration $C(x, y, t)$ in dimensionless form,

$$\frac{\partial C}{\partial t}+Pe\left(u\frac{\partial C}{\partial x}+v\frac{\partial C}{\partial y}\right)=\frac{\partial^2 C}{\partial x^2}+\frac{\partial^2 C}{\partial y^2} \tag{7}$$

where $Pe=VW/D_{cu}$ is a Péclet number, $C=\tilde{C}/C_s$ is a

dimensionless copper concentration and D_{cu} is diffusivity of copper in the slurry, which is 10^{-9} m^2/s (Zembura *et al.*, 1990). And the characteristic time is $t_c = W^2/D_{cu}$. The pad is impermeable to the dissolved copper. Therefore, the diffusive flux at the pad is zero and the initial concentration of copper in the slurry is zero. The boundary condition for copper concentration at the wafer surface is

$$\tilde{C}(x, D+d, t) = C_S, \quad -w_L \le \tilde{x} \le W + w_R \tag{8}$$

To derive the copper removal rate, we first calculated the copper concentration flux in a unit pore and then integrated the results over the pores underneath the wafer. This could be done using,

$$Removal\ rate = \frac{2 \cdot D_{cu} \cdot MW_{cu}}{\pi \cdot W \cdot R \cdot \rho_{cu}} \cdot \int_0^R \int_0^{\frac{2\sqrt{R^2 - z^2}}{V}} \int_{-w_L}^{W+w_R} \frac{\partial C}{\partial y} d\tilde{x} d\tilde{t} d\tilde{z} \tag{9}$$

where MW_{cu} is the molecular weight of copper. The two dimensional unsteady-state model is reduced to the nonlinear residual equations by applying the Galerkin finite element method. For the finite element interpolating functions, nine-node Lagrangian biquadratic basis functions are used for the concentration and velocities. Discontinuous piecewise linear basis functions defined at the centroid node of each element are used for the dynamic pressure. Typical finite element meshes for the analysis of the pore and the slurry flow field are shown in Fig. 4.

The weak forms of the field equations can be obtained by applying Galerkin FEM and divergence theorem to the mathematical model. The entire set of nonlinear algebraic equations was solved using Newton-Raphson iteration scheme and the resulting set of linear equations was solved using frontal solver developed by Hood (1976). The number of unknowns is 19,707.

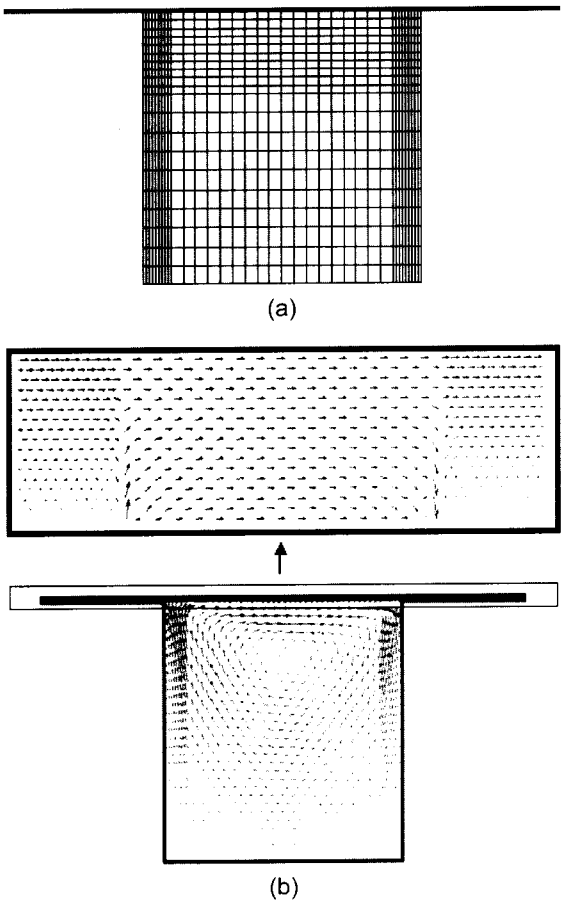

Fig. 4. (a) Finite element meshes for the numerical domain and (b) Flow field in a pore. Inset shows the magnified view of the flow in the region $\tilde{y} = D$ to $D + d$.

4. Results and discussion

Fig. 5(a) shows the concentration flux of the dissolved copper diffusing into pore along the x-directional normalized distance on the wafer surface. Because the diffusion of

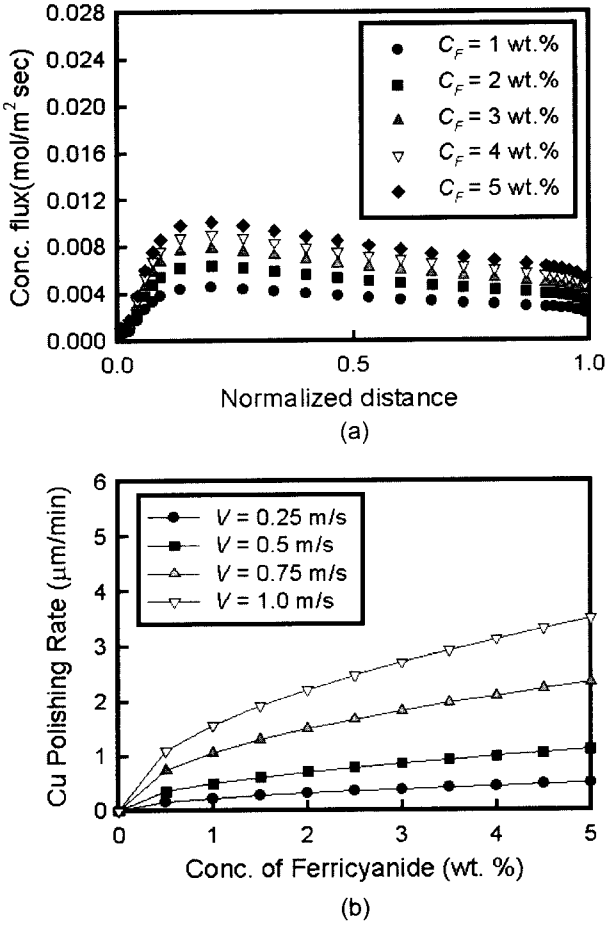

Fig. 5. Effects of concentration of chemical additives; (a) concentration flux of dissolved copper vs. x-directional scaled distance after 0.01 normalized time with C_N = 3 vol.% and V = 0.5 m/s and (b) copper removal rate vs. concentration of ferricyanide with C_N = 1 vol.%.

dissolved copper on the wafer surface means the removal of material at that site, we could anticipate the tendency of the removal rate and surface planarity in the numerical domain. At Fig. 5(a), the concentration flux increases and shows maximum value in the vicinity of 0.1 normalized distance because the slurry containing low concentration of dissolved copper is supplied through the left inlet of the pore. As the slurry moves rightwards the concentration of the dissolved copper in the slurry increases and the diffusion of the copper reduces. Fig. 5(a) also shows that the concentration flux, which can be interpreted as the removal rate of copper, is increased as the concentration of the chemical additive, ferricyanide, is increased. But we can also observe the increase of the variation of the flux along the wafer surface, which will cause the degradation of the surface planarity.

Fig. 5(b) shows the effect of the concentration of ferricyanide on the copper removal rate with the variation of the relative velocity. It is observed that the increase of ferricyanide increases the copper removal rate. And we could see that the removal rate is also proportional to the relative velocity of wafer, because the diffusion of dissolved copper is enhanced by fast slurry flow.

At the same condition of the wafer velocity and ferricyanide concentration, we compared our simulation result to the experimental data (Steigerwald, J. M. *et al.*, 1997) as shown in Fig. 6. The copper removal rate is zero in the simulation result at zero concentration of ferricyanide because copper dissolution reaction is not possible without chemicals. But in the case of experiments the removal rate is not zero, which is expected that this difference is caused by the purely mechanical abrasion effect. And as the concentration is increased the simulation result shows similar behavior to the experiment, but when the concentration is over 1 wt % we could observe that the copper removal rate of experiment does not increase as much as that of simulation result and approaches constant value. It is speculated that when the concentration of chemical additive is low the chemical dissolution reaction is rate-limiting step, that is, the amount of the chemical additive is not sufficient to dissolve out the mechanically abraded copper fragments. So the copper removal rate depends on the amount of the ferricyanide and is proportional to the concentration of

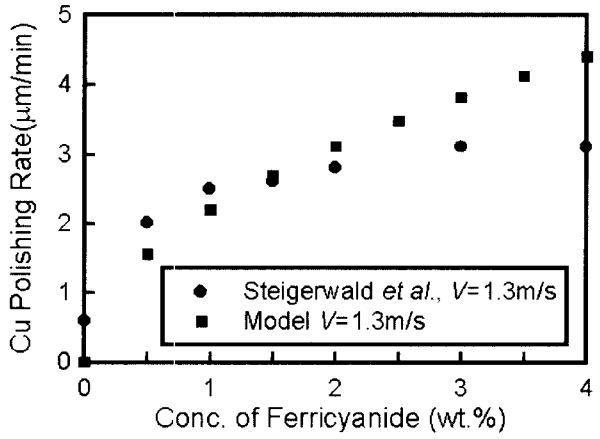

Fig. 6. Comparison of simulation result to the experimental one (Steigerwald *et al.*, 1997) with C_N = 1 vol.% and V = 1.3 m/s.

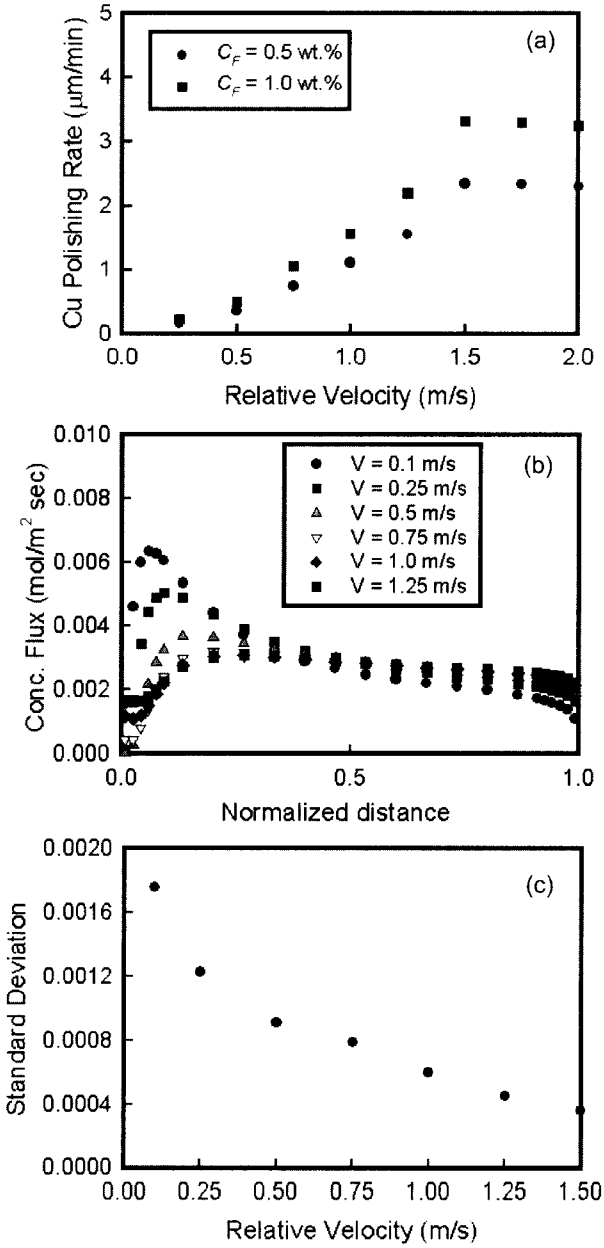

Fig. 7. Effects of relative velocity between wafer and pad; (a) copper removal rate vs. relative velocity with C_N = 1 vol. %, (b) concentration flux of dissolved copper vs. the scaled distance and (c) standard deviation of the concentration flux in the pore vs. relative velocity after 0.01 normalized time with C_N = 1 vol.% and C_F = 1 wt.%.

chemical additive. On the other hand, when the concentration of chemical additive is sufficiently high the mechanical abrasion is rate-limiting step, which means the mechanically abraded copper fragments are insufficient whereas the chemical additives are abundant in the slurry. Therefore the copper removal rate is not affected by the amount of the chemical additives. Since we did not include the mechanical effect in this study, the copper removal rate in our result is increased when the mechanical abrasion is rate-limiting step, however, we could observe that when the chemical reaction is rate-limiting step the removal rate agrees well with the experimental result. Therefore we adjusted the concentration of chemical additives below 1.5 wt.% thereafter.

Fig. 7(a) shows the effect of the relative velocity on the copper removal rate. As the velocity increases, the copper removal rate also increases at low velocity range but saturates above the critical velocity value. This saturation result shows a different behavior from the Preston equation where the removal rate is proportional to the relative velocity. The reason appears that the Preston equation mainly focuses on the mechanical abrasion effects. When the relative velocity is low, the slurry in the pore is fully saturated by the dissolved copper before the pore exits out of the wafer, which gives no contribution on the removal of copper during the remaining time exposed to the wafer. Therefore as the relative velocity is increased the removal rate is also increased because the remaining portion of wafer is chemically removed by the unsaturated slurry in the pore. But when the relative velocity is above the critical value, the slurry in the pore remains unsaturated during the time exposed to the wafer, therefore the removal rate does not increase though the relative velocity is increased.

The increase of relative velocity induces fast inflow of fresh slurry into pore containing low concentration of dissolved copper and fast outflow of slurry containing high concentration of copper. In Fig. 7(b) and 7(c) it is observed that the dissolved copper diffuses uniformly throughout the wafer when the velocity is increased, which means the increase of planarity of the wafer surface. Moreover we could observe the increase of surface planarity according to the increase of relative velocity.

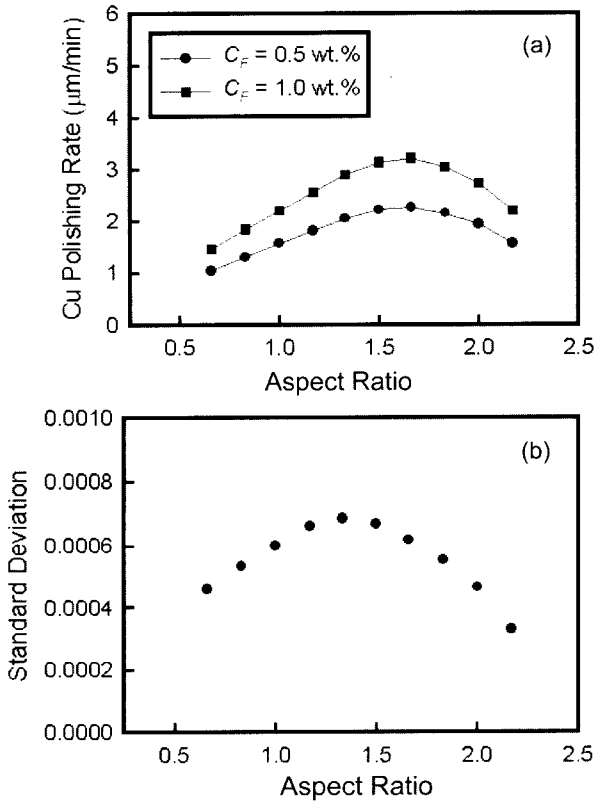

Fig. 8. Effects of pore aspect ratio on (a) copper removal rate with C_N = 1 vol.% and V = 1.0 m/s and (b) standard deviation of the concentration flux in the pore after 0.01 normalized time with C_N = 3 vol.%, C_F = 5 wt.% and V = 1.0 m/s.

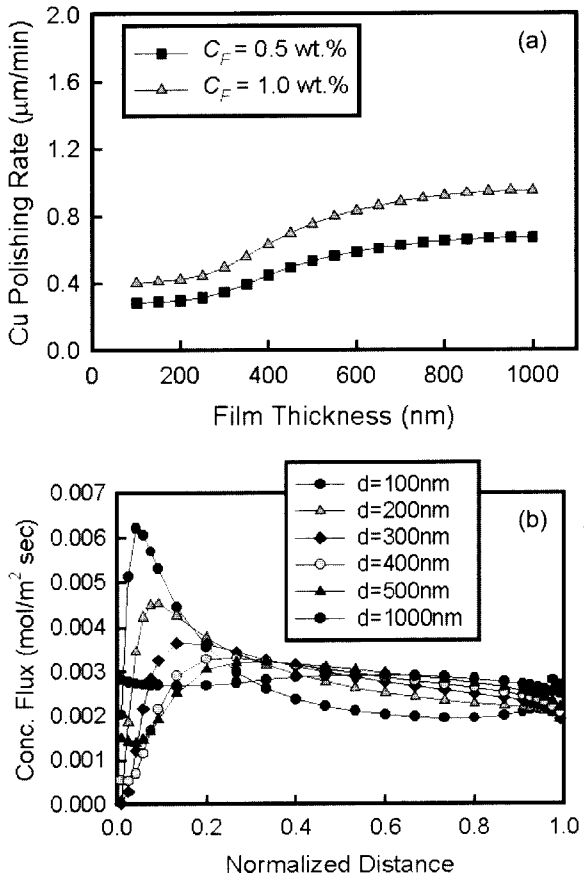

Fig. 9. Effects of slurry film thickness on (a) copper removal rate with C_N = 1 vol.% and V = 0.5 m/s and (b) concentration flux of dissolved copper along the scaled distance after 0.01 normalized time with C_N = 1 vol.%, C_F = 1 wt.% and V = 0.5 m/s.

We have investigated the effects of pore aspect ratio on the removal rate. Several pads, such as UR100 or SUBA 500 of Rodel Inc. have the pores of large aspect ratio. It is shown that the copper removal rate has the optimum value according to the aspect ratio as shown in Fig. 8(a). As the aspect ratio increases the area of the pore is also enlarged and therefore we could assume that the diffusion of dissolved copper could be more enhanced. But when the aspect ratio is larger than 1.6 a counter-rotating secondary eddy at the bottom of the pore begins to appear, which inhibits the transport of the dissolved copper material and therefore reduces the copper removal rate. And it is observed that the surface planarity also has the optimum value according to the increase of the aspect ratio as shown in Fig. 8(b).

Fig. 9 shows the effects of the slurry film thickness. The increase of the slurry film thickness induces the increase of the slurry inflow, which causes the increase of the diffusion of dissolved copper and subsequently the increase of the copper removal rate. But the removal rate saturates above critical film thickness value. It appears that this effect behaves similar to the effect of relative velocity on removal rate. Also the effect of film thickness on the surface planarity also shows similar results to that of relative velocity. In actual polishing process, the slurry film thickness is increased as the relative velocity is increased, so it is assumed to be natural to expect similar results between the effects of the relative velocity and the film thickness.

5. Conclusion

We have studied the effects of chemical reaction on the polishing rate and surface planarity in copper CMP. The increase of chemical additives, ferricyanide or ammonium hydroxide, accelerated the concentration flux of the dissolved copper because these chemical additives enhance the dissolution of copper by chemical reaction. But since the deviation of the flux along the wafer surface was also increased, the surface planarity was decreased. As the relative velocity of the wafer increased, the copper removal rate also increased at low velocity range but saturates at high velocity range above the critical value. This phenomenon was caused by the limited copper capacity of the pore. And we could observe that the uniform planarity of wafer surface was achieved when the relative velocity was increased. The copper removal rate was increased as the slurry film thickness increased more than the critical value. And the increase of slurry film thickness enhanced the surface planarity. According to the variation of the aspect ratio of pore, copper removal rate and surface planarity showed optimum values in the vicinity of 1.6 aspect ratio where the secondary counter eddy begins to appear. We can conclude that when the chemical reaction is rate-limiting step, the result of simulation matches well with the experimental data.

Acknowledgement

The authors wish to acknowledge the financial support by KIST and by the BK 21 project. Also, this research was partially funded by Center for Ultramicrochemical Process Systems sponsored by KOSEF.

References

Bhushan, M., R. Rouse and J. E. Lukens, 1995, Chemical-mechanical polishing in semidirect contact mode, *J. Electrochem. Soc.* **142**(11), 3845-3851.

Choi, D.-G., W.-J. Kim and S.-M. Yang, 2000, Shear-induced microstructure and rheology of cetylpyridinium chloride/sodium salicylate micellar solutions, *Korea-Australia Rheology Journal* **12**(3/4), 143-149.

Cook, L.M., 1990, Chemical Processes in Glass Polishing, *J. Non-Crystalline Solid* **120**, 152-171.

Hood, P., 1976, Frontal solution program for unsymmetric matrices, *International Journal for Numerical Method in Engineering* **10**, 379-399.

Kim, C., 2001, Migration in concentrated suspension of spherical particles dispersed in polymer solution, *Korea-Australia Rheology Journal* **13**(1), 19-27.

Levert, J. A., F. M. Mess, R. E. Salant, S. Danylukand and A. R. Baker, 1998, Mechanisms of chemical-mechanical polishing of SiO2 dielectric on integrated circuits, *Tribology Transactions, Soc. Tribologists and Lubrication Eng.* **41**(4), 593-599.

Preston, F. W., 1927, The theory and design of plate glass polishing machine, *J. Soc. Glass Tech.* **11**(44), 214-256.

Runnels, S. R., 1994, Feature-scale fluid based erosion modeling for chemical-mechanical polishing, *J. Electrochem. Soc.* **141**(7), 1900-1904.

Runnels, S. R., 1996, Advances in physically based erosion simulators for CMP, *J. Electronic. Mat.* **25**(10), 1574-1580.

Runnels, S. R. and L. M. Eyman, 1994, Tribology analysis of chemical-mechanical polishing, *J. Electrochem. Soc.* **141**(6), 1698-1701.

Sainio, C. A., D. J. Duquette, J. M. Steigerwald and S. P. Murarka, 1996, Eletrochemical effects in the chemical-mechanical polishing of copper for integrated circuits, *J. Electronic Materials* **25**(10), 1593-1598.

Steigerwald, J. M., S. P. Murarka and R. J. Gutmann, 1997, Chemical mechanical planarization of microelectronic materials, John Wiley & Sons, New York.

Subramanian, R., L. Zhang and S. V. Babu, 1999, Transport phenomena in chemical mechanical polishing, *J. Electrochem. Soc.* **146**(11), 4263-4272.

Sundararajan, S., D. G. Tharkurta, D. W. Schwendeman, S. P. Murarka and W. N. Gill, 1999, Two-dimensional wafer-scale chemical mechanical planarization models based on lubrication theory and mass transport, *J. Electrochem. Soc.* **146**(2), 761-766.

Sunwoo, K. B., S. J. Park, S. J. Lee, K. H. Ahn and S. J. Lee, 2000, Three-dimensional numerical simulation of nonisothermal coextrusion process with generalized Newtonian fluids, *Korea-Australia Rheology Journal* **12**(3/4), 165-173.

Sze, S.M., 1988, VLSI Technology, McGraw-Hill Companies Inc., New York.

Zembura, Z., A. Piotrowski and A. Z. Kolend, 1990, A mass-transfer model for the autocatalytic dissolution of a rotating copper disk in oxygen saturated ammonia solutions, *J. App. Electrochem.* **20**(3), 365-369.